BIOCHEMISTRY
including biophysical chemistry & molecular biology
Article

Biochemistry **2009,** *48,* 5159–5170 5159
DOI: 10.1021/bi900284x

Phospholipids Are Needed for the Proper Formation, Stability, and Function of the Photoactivated Rhodopsin−Transducin Complex[†]

Beata Jastrzebska, Anna Goc, Marcin Golczak, and Krzysztof Palczewski*

Department of Pharmacology, School of Medicine, Case Western Reserve University, Cleveland, Ohio 44106-4965

Received February 18, 2009; Revised Manuscript Received April 1, 2009

ABSTRACT: Heterotrimeric G proteins become activated after they form a catalytically active complex with activated G protein-coupled receptors (GPCRs) and GTP replaces GDP on the G protein α-subunit. This transient coupling can be stabilized by nucleotide depletion, resulting in an empty-nucleotide G protein−GPCR complex. Efficient and reproducible formation of conformationally homogeneous GPCR−Gt complexes is a prerequisite for structural studies. Herein, we report isolation conditions that enhance the stability and preserve the activity and proper stoichiometry of productive complexes between the purified prototypical GPCR, rhodopsin (Rho), and the rod cell-specific G protein, transducin (Gt). Binding of purified Gt to photoactivated Rho (Rho*) in *n*-dodecyl β-D-maltoside (DDM) examined by gel filtration chromatography was generally modest, and purified complexes provided heterogeneous ratios of protein components, most likely because of excess detergent. Rho*−Gt complex stability and activity were greatly increased by addition of phospholipids such as DOPC, DOPE, and DOPS and asolectin to detergent-containing solutions of these proteins. In contrast, native Rho*−Gt complexes purified directly from light-exposed bovine ROS membranes by sucrose gradient centrifugation exhibited improved stability and the expected 2:1 stoichiometry between Rho* and Gt. These results strongly indicate a lipid requirement for stable complex formation in which the likely oligomeric structure of Rho provides a superior platform for coupling to Gt, and phospholipids likely form a matrix to which Gt can anchor through its myristoyl and farnesyl groups. Our findings also demonstrate that the choice of detergent and purification method is critical for obtaining highly purified, stable, and active complexes with appropriate stoichiometry between GPCRs and G proteins needed for structural studies.

Heptatransmembrane helical G protein-coupled receptors (GPCRs) interact with specific heterotrimetic G proteins with appreciable affinity, but it is only after GPCR activation that these transient tight complexes are formed (*1*, *2*). Only then do G proteins become activated by the exchange of the nucleotide GDP[1] for GTP on their α-subunits. Ultimately, G proteins in turn activate their target effector molecules through either their α-subunits with bound GTP or their βγ-subunits (*3*).

The most extensively studied GPCR−G protein complex is that between rhodopsin (Rho, apoprotein opsin bound to its chromophore, 11-*cis*-retinal) and its cognate G protein, Gt or transducin (*4*). Upon exposure to a photon of light, the 11-*cis*-retinal bound covalently to Lys^{296} on transmembrane helix VII of Rho undergoes isomerizaion to all-*trans*-retinylidene, converting Rho to its activated state, Rho* (*5*, *6*). During its decay from the activated state, a single molecule of Rho binds and activates hundreds of Gt molecules, thereby propagating and markedly amplifying the light signal (*7*).

Although this description seems quite straightforward, different GPCR−G protein intermediates can be trapped. For example, the following complexes are found: complexes between Rho and Gt that form upon Rho photoactivation but in the absence of nucleotides, complexes between *cis*-retinoid regenerated Rho* and Gt in the absence of nucleotides, and complexes between opsin and Gt formed in the absence of both retinoids and nucleotides (*8*, *9*). Structural differences between these complexes remain to be defined.

[†]This research was supported in part by Grants EY008061, GM079191, and P30 EY11373 from the National Institutes of Health, Foundation Fighting Blindness, and an unrestricted grant from Amgen Inc.

*To whom correspondence should be addressed: Department of Pharmacology, School of Medicine, Case Western Reserve University, 10900 Euclid Ave., Cleveland, OH 44106-4965. Phone: (216) 368-4631. Fax: (216) 368-1300. E-mail: kxp65@case.edu.

[1]Abbreviations: AFM, atomic force microscopy; Bis-Tris propane, 1,3-bis[tris(hydroxymethyl)methylamino]propane; DDM, *n*-dodecyl β-D-maltoside; DM, *n*-decyl β-D-maltoside; DOPC, 1,2-dioleoyl-*sn*-glycero-3-phosphocholine; DOPE, 1,2-dioleoyl-*sn*-glycero-3-phosphoethanolamine; DOPS, 1,2-dioleoyl-*sn*-glycero-3-phosphoserine; DTT, dithiothreitol; HEPES, *N*-(2-hydroxyethyl)piperazine-*N*′-2-ethanesulfonic acid; HPLC, high-performance liquid chromatography; GDP, guanosine diphosphate; GTP, guanosine 5′-triphosphate; GTPγS, guanosine 5′-3-*O*-(thio)triphosphate; Gt, rod photoreceptor G protein (transducin); NG, *n*-nonyl glucopyranoside; OG, *n*-octyl glucopyranoside; PDE, phosphodiesterase; Rho, rhodopsin; Rho*, photoactivated rhodopsin or Meta II; ROS, rod outer segment(s); SDS−PAGE, sodium dodecyl sulfate−polyacrylamide gel electrophoresis; TDM, *n*-tridecyl β-D-maltoside; UDM, *n*-undecyl β-D-maltoside.

Published on Web 05/04/2009

Another factor that increases the complexity of assembly of the GPCR−G protein complex is the high density of GPCRs in native membranes that can lead to oligomerization (*10*, *11*). This can present a problem because the vast majority of experiments have been conducted in detergents that disrupt or compete with hydrophobic interactions between membrane proteins (reviewed in refs (*12*) and (*13*)). In conventional two-dimentional crystallization studies of transmembrane proteins, the typical membrane protein is present at a ratio of ~1 protein molecule per 30 phospholipids (*13*−*15*). Bacteriorhodopsin crystallizes at a 1:1 (w/w) ratio of protein to lipid (*16*); however, an increased lipid:protein ratio results in formation of aggregates without crystallization (*17*).

A specific portion of cone photoreceptor cells called cone outer segments display diffraction patterns suggesting a crystalline form of membrane-bound cone pigment complexes (*18*, *19*). Similarly, extraction of free lipids from frog rod outer segments (ROS) yields two-dimensional crystals of Rho (*20*, *21*). In mammalian ROS, Rho is packed at a ratio of 1 Rho to ~60 phospholipids or a 1:1.5 (w/w) ratio (*22*, *23*), barely more than one layer of phospholipids on average surrounding each Rho. Moreover, Rho at a concentration of 5 mM occupies 50% of the space in ROS membranes (*24*) and mimics the concentration of Rho in three-dimensional crystals. In fact, Rho crystal structures are ~70% hydrated and the protein concentration within these crystals is between 9 and 14 mM. Thus, it is hardly surprising that Rho forms heterogeneous paracrystalline assemblies in ROS (*25*−*27*). Heterogeneity of individual discs within the ROS further complicates this picture (*24*, *28*). Some imaging data are consistent with the above geometry and calculations but are inconsistent with biochemical and biophysical interpretations that assume partial or total fluidity of membranes needed for a highly diffusible receptor and G proteins to amplify light signals (reviewed in ref (*29*)). Notably, activation of a single Rho molecule suffices to trigger a physiological response, and a single Rho molecule also has been shown effectively to catalyze nucleotide exchange in Gt (*30*−*34*), even though such an ideal situation is unlikely to hold for in vivo complexes. Even if perfect separation of Rho molecules from one another is assumed, the size of the involved proteins would lead to interaction of a single Gt molecule (Gt_α, ~39 kDa), and the obligate heterodimer Gt_β (~37 kDa) and Gt_γ (~8 kDa) (*35*) with multiple Rho molecules because individual receptors protrude into the cytoplasm with ~10 kDa of protein mass separated by ~4 nm, whereas Gt spans ~7.5 nm [see modeling of the complex (*36*−*39*)]. Reduction of Rho levels in heterozygotes of Rho knockout mice reduces the size of ROS instead of decreasing Rho density (*27*), whereas an increased level of expression of Rho leads to expansion of the ROS (*40*). As a consequence of all this potential heterogeneity, it is a challenge to obtain Rho*−Gt complexes for structural studies that represent the in vivo state.

The phase distribution of GPCRs and G proteins represents yet another complexity. GPCRs are membrane proteins that require detergent solubilization for structural studies (*41*−*45*). Selection of a detergent and its concentration may have a significant influence on protein dispersion/aggregation or delipidation, and the detergent itself may bind to membrane proteins. G proteins are hydrophobic with lipophilic posttranslational modifications that are unlikely to be hydrated (*9*, *13*, *46*, *47*). Thus, extraction of such proteins from membranes for the purpose of studying complex formation and reconstitution may introduce even more heterogeneity with lipophilic modifications penetrating hydrophobic patches on proteins in an irregular fashion. So, which complexes of heterotrimeric G proteins are physiologically relevant? With the aim of answering this question, we isolated several such complexes from native ROS membranes in the presence of various detergents and extensively characterized them (*48*). Here we report how these structures compare with complexes formed from purified components and also document a possible role for phospholipids in these complexes and the effects of different detergents upon them. Phospholipids appear to be indispensible for the activity, stability, and proper stoichiometry of various Rho−Gt complexes.

MATERIALS AND METHODS

Chemicals. Guanosine 5′-3-*O*-(thio)triphosphate (GTPγS) was purchased from Sigma (St. Louis, MO). *n*-Octyl glucopyranoside (OG), *n*-nonyl glucopyranoside (NG), *n*-decyl β-D-maltoside (DM), *n*-undecyl β-D-maltoside (UDM), *n*-dodecyl β-D-maltoside (DDM), and *n*-tridecyl β-D-maltoside (TDM) were obtained from Anatrace Inc. (Maumee, OH). Bradford ULTRA was purchased from Novexin (Cambridge, U.K.). Asolectin was procured from Sigma. 1,2-Dioleoyl-*sn*-glycero-3-phosphocholine (DOPC), 1,2-dioleoyl-*sn*-glycero-3-phosphoethanolamine (DOPE), and 1,2-dioleoyl-*sn*-glycero-3-phosphoserine (DOPS) were obtained from Avanti Polar Lipids (Alabaster, AL).

Purification of Rho. Bovine ROS membranes were prepared from fresh retinas under dim red light according to the Papermaster procedure (*49*). Rho was solubilized in DDM and purified from ROS by the $ZnCl_2$−opsin precipitation method that yields Rho with an A_{280}/A_{500} absorbance ratio of 1.63 (*42*). $ZnCl_2$ was removed by dialysis in the presence of 0.1% DDM. Rho concentrations were determined with a Cary 50, UV−visible spectrophotometer (Varian, Palo Alto, CA) and quantified by absorption at 500 nm by using an absorption coefficient ε of 40600 M^{-1} cm^{-1} (*50*).

Purification of Gt. Bovine ROS membranes were prepared from 100 frozen retinas (W. L. Lawson Co., Lincoln, NE) under dim red light. Gt was purified according to a procedure described elsewhere (*9*). Briefly, ROS membranes were diluted in 10 mL of isotonic buffer [20 mM HEPES (pH 7.5), 5 mM $MgCl_2$, 1 mM DTT, and 100 mM NaCl], and soluble proteins were removed by gentle homogenization followed by centrifugation at 25000*g* and 4 °C for 15 min. Gt then was extracted from the pellet in 10 mL of hypotonic buffer [5 mM HEPES (pH 7.5), 0.1 mM EDTA, and 1 mM DTT]; membranes were collected by centrifugation at 25000*g* and 4 °C for 45 min, and the supernatant was saved for further purification. This extraction procedure was repeated three times. Combined supernatants were centrifuged at 25000*g* for 60 min to remove ROS membrane contaminants and dialyzed overnight at 4 °C against equilibrating buffer [10 mM HEPES (pH 7.5), 2 mM $MgCl_2$, and 1 mM DTT]. This solution was applied at a flow rate of 15 mL/h to a 10 mm × 100 mm column with 3 mL of pre-equilibrated propyl-agarose resin, and the column was washed with 5 column volumes of equilibrating buffer. Bound proteins were eluted with a 50 mL linear gradient from 0 to 0.5 M NaCl in equilibrating buffer at a flow rate of 15 mL/h, and 1 mL fractions were collected. Fractions containing Gt were pooled, dialyzed overnight at 4 °C against 10 mM HEPES (pH 7.5) containing 2 mM $MgCl_2$, 1 mM DTT, and 100 mM NaCl, and then concentrated with 30000 NMWL Centricon devices (Millipore, Billerica, MA). Gt was purified

to homogeneity on a Superdex 200 gel filtration column equilibrated with dialysis buffer at 4 °C; the flow rate was 0.4 mL/min, and 0.4 mL fractions were collected. Fractions containing Gt were combined and concentrated with 30000 NMWL Centricon devices to ~10 mg of protein/mL, determined by the Bradford assay (*51*).

Binding of Gt to Rho Examined by Gel Filtration Chromatography*. Gt bound to Zn^{2+}-extracted Rho under a variety of conditions (different Rho*:Gt molar ratios, in different detergents, and with added phospholipids or NH_2OH), and the resulting complexes were analyzed after size exclusion chromatography on a Superdex 200 10/300 GL column (Amersham Biosciences, Piscataway, WI), with a FPLC instrument (DuoFlow System, Bio-Rad, Hercules, CA). The column was run at 4 °C with a solution composed of 20 mM BTP buffer (pH 6.9) containing 120 mM NaCl, 2 mM $MgCl_2$, 1 mM DTT, and 1 mM DDM for all experiments conducted in the presence of DDM. For testing of other detergents, the solution contained either 13 mM NG, 3.6 mM DM, 2.3 mM UDM, or 0.5 mM TDM. Columns were run at a flow rate of 0.4 mL/min at 4 °C, and 0.4 mL fractions were collected. Rho (200 μg) was mixed with 100 μg of Gt in 20 mM BTP buffer (pH 6.9) containing 120 mM NaCl, 2 mM $MgCl_2$, 1 mM DTT, and 1 mM DDM, bleached for 5 min by a Fiber-Light covered with a 480−525 nm band-pass filter (Chroma Technology, Rockingam, VA) at a distance of 10 cm, and incubated on ice for 15 min to form the complex. Proteins then were loaded onto a gel filtration column at 4 °C equilibrated with 20 mM BTP (pH 6.9) containing 120 mM NaCl, 2 mM $MgCl_2$, 1 mM DTT, and 1 mM DDM. Control gel filtration chromatography experiments were performed with either free Rho and free Gt, a mixture of nonactivated Rho and Gt, or a mixture of Rho and Gt and freshly neutralized 10 mM NH_2OH that was light activated to accomplish Schiff base hydrolysis. Dissociation of Gt from the complex with light-activated Rho* was analyzed by adding 200 μM GTPγS (Roche Diagnostics, Indianapolis, IN) after complex formation. After incubation for 30 min on ice, proteins were loaded onto a gel filtration column equilibrated with 5 mM BTP (pH 6.9) containing 10 mM NaCl, 2 mM $MgCl_2$, 1 mM DTT, 1 mM DDM, and 10 μM GTPγS. Columns were run at a flow rate of 0.4 mL/min at 4 °C, and 0.4 mL fractions were collected.

The influence of different Rho* and Gt ratios on complex formation was investigated by mixing different amounts of both proteins together to attain the following Rho*:Gt molar ratios: 12.5 μg of Rho and 100 μg of Gt (1:4), 100 μg of Rho and 200 μg of Gt (1:1), 200 μg of Rho and 200 μg of Gt (2:1), and 200 μg of Rho and 100 μg of Gt (4:1). Proteins were mixed in a buffer composed of 20 mM BTP (pH 6.9) containing 120 mM NaCl, 2 mM $MgCl_2$, 1 mM DTT, and 1 mM DDM and then illuminated for 5 min by using a Fiber-Light covered with a 480−525 nm band-pass filter at a distance of 10 cm. After incubation for 15 min on ice, protein samples were loaded onto gel filtration columns equilibrated with 20 mM BTP (pH 6.9) containing 120 mM NaCl, 2 mM $MgCl_2$, 1 mM DTT, and 1 mM DDM. Columns were run at a flow rate of 0.4 mL/min at 4 °C, and 0.4 mL fractions were collected.

For testing the influence of lipids (asolectin, DOPC, DOPE, and DOPS) on binding of Gt to photoactivated Rho*, samples containing Rho and Gt mixtures were incubated with phospholipids in 20 mM BTP (pH 6.9) containing 120 mM NaCl, 2 mM $MgCl_2$, 1 mM DTT, and 1 mM DDM. Asolectin and DOPC, DOPE, and DOPS were added to attain a 1:100 Rho:lipid ratio. After incubation for 1 h at room temperature, samples were illuminated and loaded onto gel filtration columns equilibrated with buffer composed of 20 mM BTP (pH 6.9) containing 120 mM NaCl, 2 mM $MgCl_2$, 1 mM DTT, and 1 mM DDM. Columns were run at a flow rate of 0.4 mL/min at 4 °C, and 0.4 mL fractions were collected.

*Gt Activation by Rho**. Activation of Gt was tested as previously described (*52*). Briefly, purified Gt (250 nM) was added to Rho (25 nM) in 20 mM BTP (pH 7.0) containing 120 mM NaCl, 5 mM $MgCl_2$, and 1 mM DDM. We used Zn^{2+}-extracted Rho with or without added phospholipids such as DOPC, DOPE, DOPS, or those extracted from ROS membranes. Rho was incubated with phospholipids (Rho:lipid molar ratio of 1:100) for 2 h at room temperature in the buffer described above. Gt was activated by Rho* in ROS membranes for the control experiment. Samples were bleached for 30 s with a Fiber-Light covered with a 480−525 nm band-pass filter (Chroma Technology, Rockingham, VT), followed by a 5 min incubation with continuous low-speed stirring. Then 5 μM GTPγS was added, and the intrinsic fluorescence of Gt_α was measured with an LS55 luminescence spectrophotometer (Perkin-Elmer, Waltham, MA), by using excitation and emission wavelengths of 300 and 345 nm, respectively (*53*, *54*). The fluorescence change was linear within the range of protein concentrations used. No fluorescence signal was detected in the control experiment without GTPγS.

Isolation of the Native Rho−Gt Complex by Sucrose Gradient Ultracentrifugation*. The native Rho*−Gt complex was isolated from bovine retinas according to the procedure described by Jastrzebska et al. (*48*). ROS membranes (0.2 mg/mL protein) were suspended in 20 mM BTP (pH 6.9) containing 120 mM NaCl, 0.1 mM $MgCl_2$, and 1 mM DTT, bleached for 10 min at a distance of 10 cm under a Fiber-Light covered with a 480−525 nm band-pass filter, and incubated for 15 min on ice. To remove soluble proteins present in ROS and endogenous GDP released from the Gt nucleotide-binding site, ROS membranes were washed five times with 5 mM BTP (pH 6.9) containing 0.1 mM $MgCl_2$ and 1 mM DTT followed by a single wash with 20 mM BTP (pH 6.9) containing 120 mM NaCl, 0.1 mM $MgCl_2$, and 1 mM DTT. The Rho*−Gt complex then was solubilized with 20 mM BTP (pH 6.9) containing 120 mM NaCl, 0.1 mM $MgCl_2$, 1 mM DTT, and 20 mM DDM for 1 h on ice (*8*). Insoluble material removed by centrifugation at 100000*g* for 1 h was discarded. Alternatively, samples were solubilized in different detergents such as 50 mM OG, 50 mM NG, 20 mM DM, 20 mM UDM, or 20 mM TDM. The Rho*−Gt complex was enriched by using a 750 μL−900 μL−900 μL−750 μL step gradient composed of 20%−30%−40%−50% sucrose in 20 mM BTP (pH 6.9) containing 120 mM NaCl, 0.1 mM $MgCl_2$, 1 mM DTT, and 0.3 mM DDM. The density of each fraction was determined from its refractive index. The detergent-solubilized Rho*−Gt complex (300 μL, 2 mg/mL protein) was loaded atop the gradient and centrifuged at 269000*g* for 16 h, and fractions (250 μL each) were collected from the top to the bottom of the gradient. The protein content in these fractions was analyzed by SDS−PAGE and immunoblotting. As controls for these experiments, described above, 50 μg of purified Rho (*42*) and 50 μg of purified Gt (*9*) were suspended in 20 mM BTP (pH 6.9) containing 120 mM NaCl, 0.1 mM $MgCl_2$, and 1 mM DTT (100 μL total volume) and subjected to sucrose gradient centrifugation after either being kept in the dark or exposed to illumination.

Quantification of Total Phospholipids. Total phospholipids in Rho*−Gt complexes isolated either by gel filtration chromatography or by sucrose gradient ultracentrifugation were

quantified by phosphorus analysis (*55*). Fractions 28−32 containing no phospholipids or a mixture of DOPC and DOPE, fractions 26−30 containing DOPS obtained after gel filtration chromatography (Figures 1A and 3), and fractions 6−8 obtained after sucrose gradient centrifugation (Figure 6) were collected for phospholipid quantification. Phospholipids were extracted with a methanol/$CHCl_3$ solution mixed in a 2:5 ratio, dried down in a Speed Vac, and then redissolved in $CHCl_3$. The $CHCl_3$ solution was separated into three different lipid classes (neutral lipids, glycolipids, and polar lipids) by silica acid column chromatography and subsequently eluted with $CHCl_3$, acetone, and methanol (*56*). The methanol fraction containing phospholipids was dried down and redissolved in a 10% H_2O/80% methanol/10% $CHCl_3$ mixture. Sixty percent perchloric acid (650 μL) was added to 90 μL of sample and heated for 2 h at 100 °C to hydrolyze phospholipids. Then 3.4 mL of H_2O, 0.5 mL of 2.5% ammonium molybdate, and 0.5 mL of 10% ascorbic acid were added to the sample and incubated for 30 min. Absorption was measured at 797 nm, and the phosphate content in the sample was calculated from a standard calibration curve.

Determination of Molar Ratios between Rho and Gt in Isolated Rho*−Gt Complexes*. Ratios of Gt_α, Gt_β, and Rho* in fractions containing Rho*−Gt complexes purified by either gel filtration or sucrose gradient ultracentrifugation were calculated from gels stained with Coomassie blue by using Image J (http://rsb.info.nih.gov/ij/ and http://www.uhnresearch.ca/facilities/wcif/imagej/).

RESULTS

Formation of the Reconstituted Rho−Gt Complex*. Purified proteins were used to reconstitute the complex between Rho and Gt. Rho was purified by opsin Zn^{2+} extraction as described in Materials and Methods. Sample purity was determined by its absorption spectra and Coomassie-blue stained gels [Figures S1A and S1C of the Supporting Information (inset)]. Typically, this purification procedure yielded Rho with an absorption at 280 nm:absorption at 500 nm ratio of ~1.6 (Figure S1A, black line) that displayed typical behavior under dark and light conditions. Light illumination activated Rho and stimulated formation of Meta II (Figure S1A, gray line), retaining the attached chromophore as recognized by protonation of the Schiff base with acid, and a shift in maximum absorption from 380 to 440 nm (Figure S1A, light gray line). However, in the presence of NH_2OH after light illumination, the chromophore was hydrolyzed from its binding pocket; therefore, there was no shift of the absorption maximum (Figure S1B, gray and light gray line). Gt was purified as described in Materials and Methods, and its purity was examined by Coomassie-blue stained gels [Figure S1C (inset)]. Formation of the complex between Rho* and Gt was examined by a fluorescence-based assay that involves monitoring guanylyl nucleotide exchange in the α-subunit of Gt that occurs upon its activation by Rho* (Figure S1C). The typical change in the intrinsic fluorescence of Gt_α because of nucleotide exchange stimulated by Rho* was observed. The determined rate of activation was similar to rates previously reported under comparable experimental conditions (*52*, *57*).

Gel Filtration of Reconstituted Rho−Gt Complexes*. Binding of purified Gt to Rho* in DDM was examined by gel filtration chromatography (Figure 1). Upon formation of Rho*, Gt binds to the receptor's cytoplasmic surface (*58*), forming a protein complex with a molecular mass higher than those of its

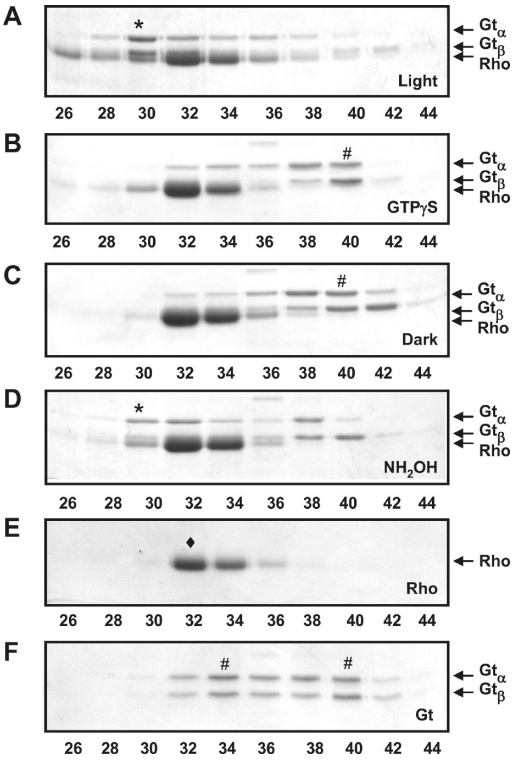

FIGURE 1: Gel filtration of reconstituted Rho*−Gt complexes in DDM under various experimental conditions indicated in the bottom right corner of each panel. (A) Gel filtration of Gt and Rho exposed to light. (B) Dissociation of Gt from the Rho*−Gt complex after addition of GTPγS. (C) Gel filtration of a Rho and Gt mixture in the dark. (D) Gel filtration of Gt and Rho exposed to light in the presence of NH_2OH. (E) Gel filtration of free Rho. (F) Gel filtration of free Gt. Fractions (30 μL) were analyzed by Coomassie blue-stained SDS−PAGE. Asterisks denote fractions containing the Rho*−Gt complex. Number signs denote fractions containing free Gt. The diamond denotes the fraction containing free Rho. Presented gels are representative of three independent experiments.

two protein components. Thus, the Rho*−Gt complex should migrate faster on size exclusion chromatography. Although the molecular mass of Gt is 83 kDa (39 kDa α-subunit, 36 kDa β-subunit, and 8 kDa γ-subunit) (*58*), purified Gt eluted from the gel filtration Superdex 200 column in the presence of DDM spread through fractions 32−42 with higher concentrations in fractions 34 and 40 (Figure 1F). This might suggest that there are two populations of Gt, i.e., bound and not bound to detergent micelles. Free Rho migrated mainly in fractions 32−34 (Figure 1E). When the mixture of Rho and Gt was applied to the gel filtration column and eluted in the dark, most of the Gt was present in fractions 36−42. However, some Gt was detected in fractions 32−34, most likely because it bound to the detergent micelles, although precoupling to ground state Rho cannot be excluded (Figure 1C). Complexes of Gt and Rho with higher molecular masses appeared in earlier fractions 28−30 (Figure 1A). Addition of GTPγS, a nonhydrolyzable analogue of GTP, led to release of Gt_α and $Gt_{\beta\gamma}$ subunits from Rho*, visible as a shift of Gt to the later 38−40 fractions (Figure 1B). Addition of the nucleophile NH_2OH, which promotes release of the chromophore from the Rho ligand binding pocket after light activation, did not affect formation of the complex between opsin and Gt that mostly appeared in fraction 30, similar to the same complex formed in the absence of NH_2OH (compare panels A and D of Figure 1). Although formation of the Rho*−Gt complex after light activation was detected, its concentration was low, either because of

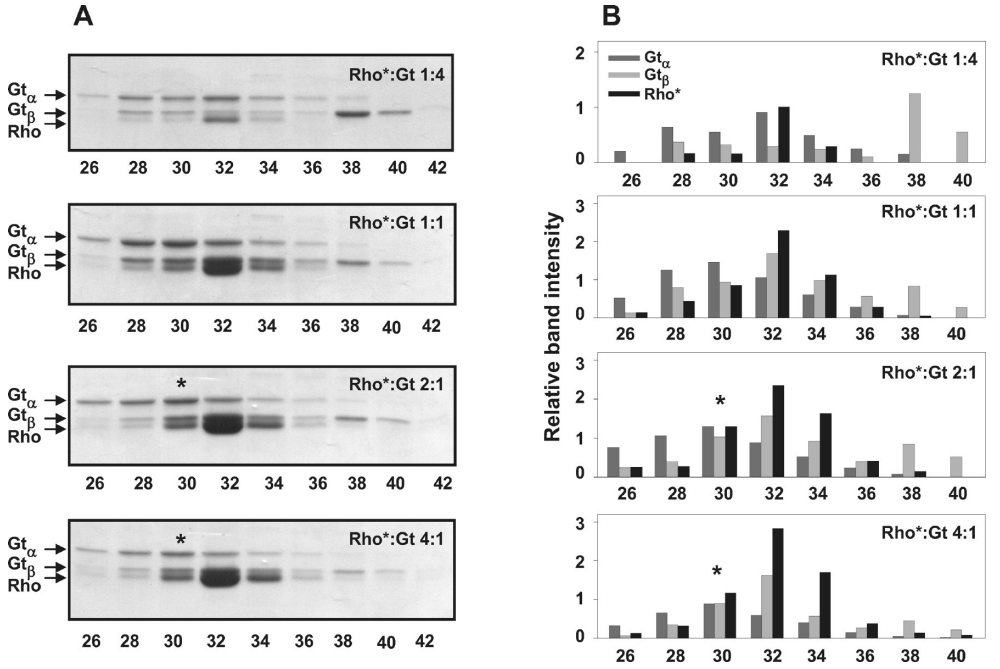

FIGURE 2: Gel filtration of Rho*−Gt complexes obtained by mixing Rho and Gt together at different molar ratios (1:4, 1:1, 2:1, and 4:1). (A) Fractions (30 μL) were analyzed by Coomassie blue-stained SDS−PAGE. Asterisks denote fractions containing the Rho*−Gt complex. (B) Quantification of band intensities corresponding to Gt_α, Gt_β, and Rho* in fractions collected from the gel filtration column. Asterisks denote fractions containing a 1:1 molar ratio of Rho* to Gt. The results suggest that an excess of Rho in the original sample results in formation of a 1:1 Rho*−Gt complex. Presented gels are representative of three independent experiments.

poor complex formation or, more likely, because the complex stability was affected by the presence of detergent.

To determine if the stability of the complex is regulated by the ratio of Rho to Gt, several different ratios of these two purified proteins were mixed together (1:4, 1:1, 2:1, and 4:1 Rho:Gt) and subjected to gel filtration after photoactivation (Figure 2). This experiment revealed that an excess of Rho, either 2:1 or 4:1, provided higher yields of the complex and that the complex with a 1:1 Rho*:Gt ratio was present mostly in fraction 30 (Figure 2A,B, asterisks, two bottom panels). When Rho and Gt were mixed in the presence of an excess or equivalent ratio of Gt to Rho, an ~5-fold molar excess of Gt compared to Rho* was detected in fraction 30 (Figure 2A,B, top two panels). Some free Gt_β was detected in fractions 38−42, suggesting that photoactivated Rho* causes partial dissociation of the $Gt_{\beta\gamma}$ subunit.

Influence of Phospholipids on Formation and Stability of the Rho−Gt Complex*. Many published reports suggest that a dimer is the structural unit of Rho that forms the interface for Gt binding. Because it is possible that detergent might destabilize the interaction between Rho and Gt, we tested whether exogenous phospholipids could affect this interaction. The Rho*−Gt complex was prepared from purified proteins, and phospholipids such as DOPC, DOPE, DOPS, and asolectin were added at a ratio of 100 molecules per Rho molecule (Figure 3). The presence of phospholipids shifted migration of the Rho*−Gt complex to earlier, heavier fractions and enriched these fractions with Rho*. However, quantification of Rho* and Gt content in peak fractions containing the Rho*−Gt complex indicated a ratio of ~3:1 for all tested phospholipids except asolectin, suggesting an excess of Rho*. Thus, it appears that phospholipids stabilize complex formation and/or Rho oligomeric assembly. To explore this question, free Rho was subjected to gel filtration in the presence of phospholipids and its migration was compared with that of Rho without added phospholipids (Figure S2 of the Supporting Information). In this case, phospholipids enhanced the migration of Rho, indicating its presence in heavier particles, presumably as oligomers in mixed detergent/lipid micelles. This experiment does not eliminate the possibility of stabilization of the Rho*−Gt complex, but the quantified ratios suggest the presence of excess Rho* contaminating fractions containing the Rho*−Gt complex. Free Gt_β was detected in fractions 40−42, suggesting that photoactivated Rho* causes partial dissociation of the $Gt_{\beta\gamma}$ subunit.

Phospholipids then were quantified in fractions containing the reconstituted Rho*−Gt complex obtained after gel filtration of samples either without added phospholipids or containing exogenously added DOPS or a mixture of DOPC and DOPE (Figure 4). Approximately 5 times more phospholipids were found in fractions from samples of the reconstituted Rho*−Gt complex incubated with phospholipids prior to loading the gel filtration column (Figure 4), suggesting that Rho is naturally incorporated into phospholipids present in detergent/lipid mixed micelles. Significantly, gel filtration of the native Rho*−Gt complex without added phospholipids resulted in purified fractions of this complex that contained substantially more lipid (>2-fold, ~16 phospholipids per Rho) than comparable fractions of the reconstituted complex (~6 phospholipids per Rho), whereas purification of the native complex by sucrose gradient centrifugation resulted in purified Rho*−Gt complexes that retained lipid in amounts comparable to the amounts of reconstituted complexes with added phospholipids purified by gel filtration (~30 phospholipids per Rho) (Figure 4).

Phospholipids also were shown to be critical for optimal Gt activation (Figure 5). Activation rates were faster in the presence of lipids and depended on the type of lipid present. Rho incorporated into DOPS had a far greater effect on the Gt activation rate than it did in the presence of either DOPC or DOPE, resulting in 15-fold faster activation than purified Rho* in detergent micelles; activation in the presence of DOPC and DOPE was 3.4 and 1.8 times faster, as well. Rho incorporated

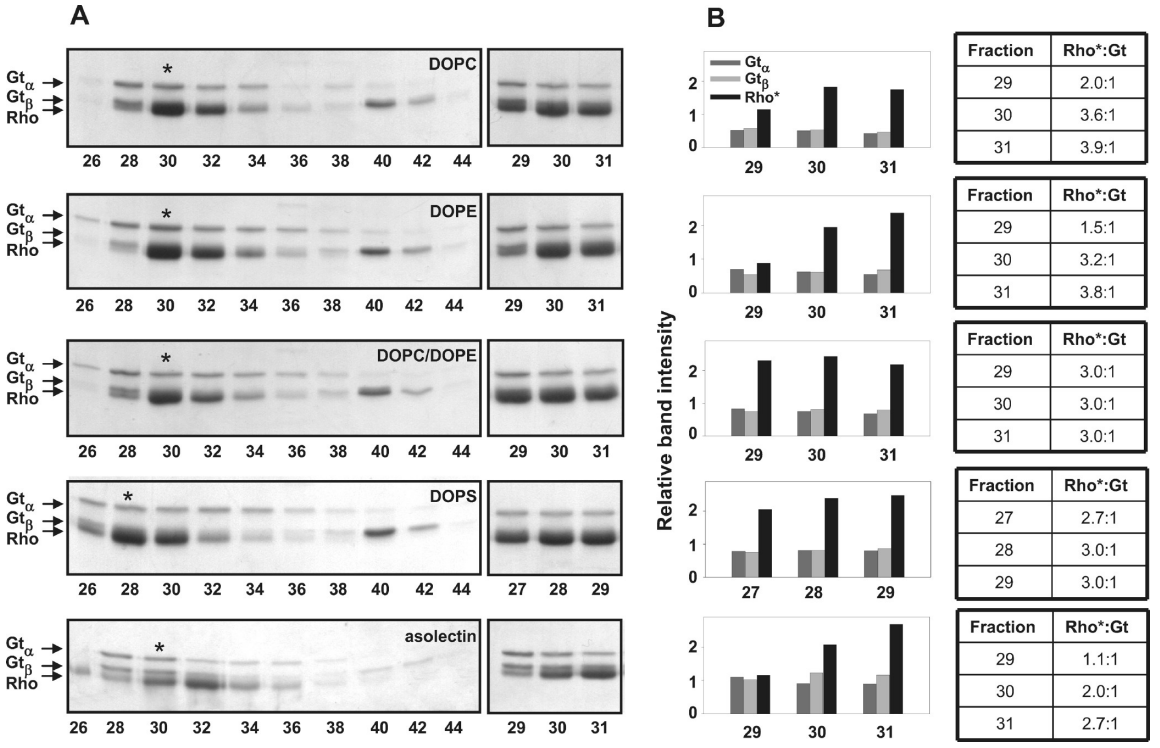

FIGURE 3: Gel filtration of Rho*−Gt complexes in the presence of phospholipids at a Rho:lipid molar ratio of 1:100. DOPC, DOPE, a 1:1 mixture of DOPC and DOPE, DOPS, and asolectin were examined. (A) Fractions (30 μL) obtained from gel filtration analyzed by Coomassie blue-stained SDS−PAGE. Asterisks denote fractions containing the highest concentration of Rho*−Gt complex. (B) Quantification of band intensities corresponding to Gt_α, Gt_β, and Rho* in peak fractions containing the Rho*−Gt complex (right panels) and calculated Rho*:Gt molar ratios in these fractions (tables, left panels). Results indicate that phospholipids increase the content of Rho in fractions containing the Rho*−Gt complex, resulting in molar ratios of Rho* to Gt of >3; however, asolectin provided a ratio of $\sim$2. Presented gels are representative of three independent experiments.

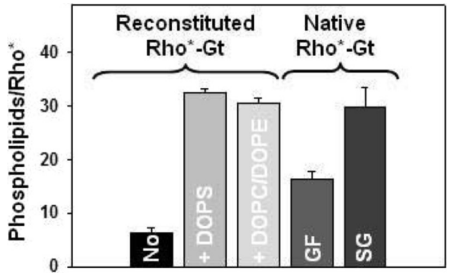

FIGURE 4: Phospholipid:Rho* ratios in fractions of reconstituted Rho*−Gt complexes isolated by gel filtration either without (No) or with prior addition of phospholipids (DOPS or DOPC/DOPE) (left). Phospholipid:Rho* ratios in fractions of native Rho*−Gt complexes isolated either by gel filtration (GF) or by sucrose gradient ultracentrifugation (SG) are shown (right). Average numbers of phospholipid molecules per single Rho molecule were calculated from three independent experiments.

into phospholipids extracted from ROS membranes activated Gt at a rate similar to that of native Rho in ROS membranes and $\sim$7−9 times faster than the rate for Rho solubilized in detergent alone. These results strongly indicate the necessity of phospholipids for rapid signal propagation in photoreceptor cells. Phospholipids most likely affect Rho oligomerization (*59*), providing a better platform for coupling with Gt as well as a matrix for Gt anchorage by its myristyl and farnesyl groups.

Isolation of the Native Rho−Gt Complex*. Because isolation of the reconstituted Rho*−Gt complex by size exclusion chromatography did not yield a homogeneous complex with a well-defined ratio between Rho* and Gt, we developed a method for purifying the native Rho*−Gt complex. In vivo, binding of Gt to Rho* occurs in native ROS membranes where Rho is properly organized in a lipid bilayer. After washing and membrane solubilization, we used a four-step gradient of sucrose (20%−30%−40%−50%) to separate the Rho*−Gt complex by ultracentrifugation. Fractions of 250 μL were collected from the top to bottom of the gradient, and the protein content of each fraction was determined by Coomassie blue-stained SDS−PAGE and immunoblots (Figure 6). After overnight ultracentrifugation, the Rho*−Gt complex was found in fractions 6−8 containing 30−40% sucrose where it was highly enriched but not homogeneous. (Figure 6A). To determine if the complex was biochemically active, 200 μM GTPγS was added to samples before they were loaded on the sucrose gradient. Most of the complex dissociated, and Rho* and the Gt−GTPγS complex were found mainly in fractions 3−5 containing 20−25% sucrose (Figure 6B), the same fractions that contained free Rho and free Gt in the control experiment (Figure 6C). The molar ratio between Rho* and Gt quantified in fractions 6−8 was 2:1 (Figure 6D). These results strongly suggest that native phospholipids present in the sample or the method used for isolation of the Rho*−Gt complex can stabilize the complex in a well-defined 2:1 Rho*:Gt molar ratio.

We then compared the effectiveness of sucrose gradient ultracentrifugation and gel filtration chromatography in isolating the native complex (Figure 7). The native Rho*−Gt complex was prepared in ROS membranes as described above, but solubilized membranes were loaded onto a gel filtration column instead of a sucrose gradient. Most of the Rho*−Gt complex appeared in fraction 30, whereas excess free photoactivated Rho* eluted in subsequent fractions (Figure 7A). The isolated complex was functional in that it could be dissociated

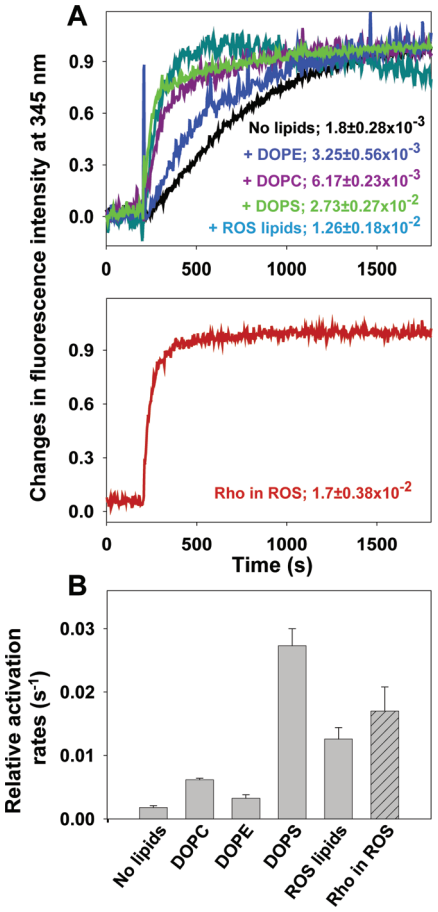

FIGURE 5: Intrinsic fluorescence increase of the Gt_α subunit caused by interaction with photoactivated Rho* without and with addition of synthetic phospholipids or lipids isolated from ROS membranes. Zn^{2+}-extracted Rho (25 nM) was mixed with phospholipids at a 1:100 molar ratio in buffer composed of 20 mM BTP (pH 7.0) containing 120 mM NaCl, 5 mM $MgCl_2$, and 1 mM DDM and incubated for 2 h at room temperature. Then Gt was added (250 nM), and samples were illuminated for 30 s. After data had been recorded for 300 s, 5 μM GTPγS was added. Reactions were conducted in the buffer described above at 20 °C in continuously stirred cuvettes. When Gt was activated by ROS membranes, DDM was omitted from the reaction buffer. (A) Activation of Gt by Rho* without added phospholipids (black line), in the presence of DOPE (blue line), in the presence of DOPC (purple line), in the presence of DOPS (green line), and in the presence of lipids isolated from ROS membranes (dark cyan line) (top panel). Activation of Gt by Rho* in ROS membranes (red line) (bottom panel). Relative activation rates were calculated from three independent experiments. (B) Comparison of the relative activation rates. Rates of Gt activation were greater in the presence of phospholipids, suggesting an important role of lipids in the Rho*−Gt signaling complex.

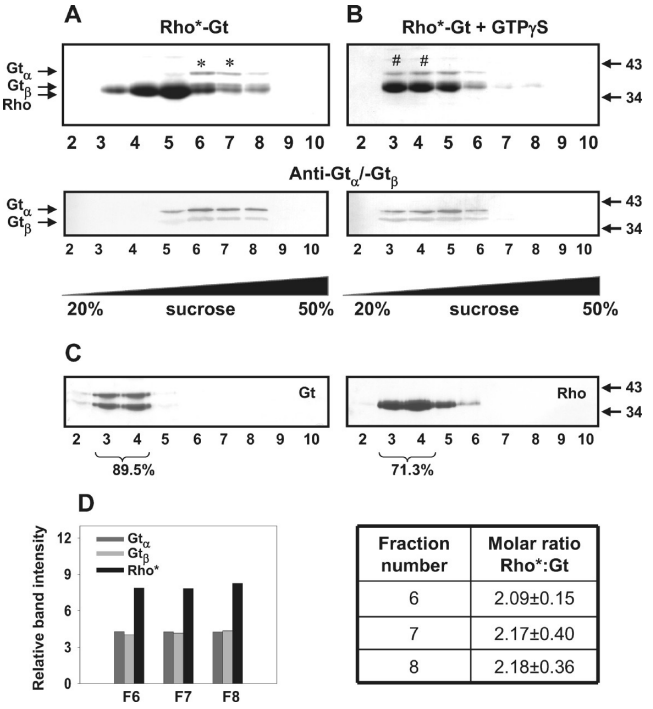

Fraction number	Molar ratio Rho*:Gt
6	2.09±0.15
7	2.17±0.40
8	2.18±0.36

FIGURE 6: Isolation of the native Rho*−Gt complex solubilized in DDM by sucrose gradient ultracentrifugation. Fractions 1−13 (250 μL each) were collected from the top to bottom of a sucrose gradient after overnight ultracentrifugation as described in Materials and Methods. Fifteen microliters of each fraction was analyzed by Coomassie blue-stained SDS−PAGE (top panels) or immunoblots developed with a mixture of anti-Gt_α and anti-Gt_β antibodies (bottom panels). (A) Separation of the Rho*−Gt complex from excess Rho*. Asterisks denote fractions containing the highest concentrations of the Rho*−Gt complex. (B) Dissociation of the Rho*−Gt complex by 200 μM GTPγS. Number signs denote fractions dissociated by the Gt−GTPγS complex. (C) Control separation of free Gt (left panel) and detergent-solubilized Rho (right panel) by sucrose gradient ultracentrifugation. (D) Quantification of band intensities corresponding to Gt_α, Gt_β, and Rho* (left) and calculations of Rho*:Gt molar ratios in fractions containing the Rho*−Gt complex (right). Preparation of the Rho*−Gt complex in native lipid-containing membranes and its purification by sucrose gradient ultracentrifugation appear to be important for the stability and proper stoichiometry of this complex. Experiments were repeated at least three times.

by GTPγS that shifted free Gt into later fractions with a peak in fraction 36. The molar ratio between Rho* and Gt in the complex isolated in fraction 30 was ~1:1. This result suggests that during gel filtration more phospholipids surrounding Rho* are sequestered and that their loss most likely causes disruption of the Rho dimeric organization. This result contrasts with that found after sucrose gradient purification where the protein sample is not exposed to a high volume of detergent-containing buffer disrupting the lipid environment protecting Rho. To check this hypothesis, we compared the phospholipid content of the native Rho*−Gt complex purified either by sucrose gradient centrifugation or by gel filtration (Figure 4). In fact, ~30 phospholipid molecules per one molecule of Rho* were found in fractions of the complex sample purified by sucrose gradient ultracentrifugation, whereas only 16 phospholipid molecules per Rho* molecule were found in the fractions purified by gel filtration.

Influence of Detergent on the Stability of the Rho−Gt Complex*. To examine effects of different detergents on the properties of the Rho*−Gt complex purified from native ROS, we tested several detergents, including OG, NG, DM, UDM, and TDM, and compared the results with those obtained with DDM (Figure 8). The Rho*−Gt complex in native ROS membranes was prepared as described above but solubilized in one of these detergents and then isolated by sucrose gradient ultracentrifugation. All four alkyl maltoside detergents seemed to affect complex isolation in a manner similar to that of DDM such that the Rho*−Gt complexes appeared mostly in fractions 6−8. In contrast, detergents such as OG and NG that are commonly used to extract membrane proteins had destructive effects on the complex stability. Rho* and Gt were distributed broadly in fractions 6−11, suggesting that different heavier complexes were formed and/or aggregated. Some free Rho* and Gt_β was also found in fractions 3−5. Possibly, alkyl glucosides are unable to solubilize sufficient phospholipids to maintain a proper

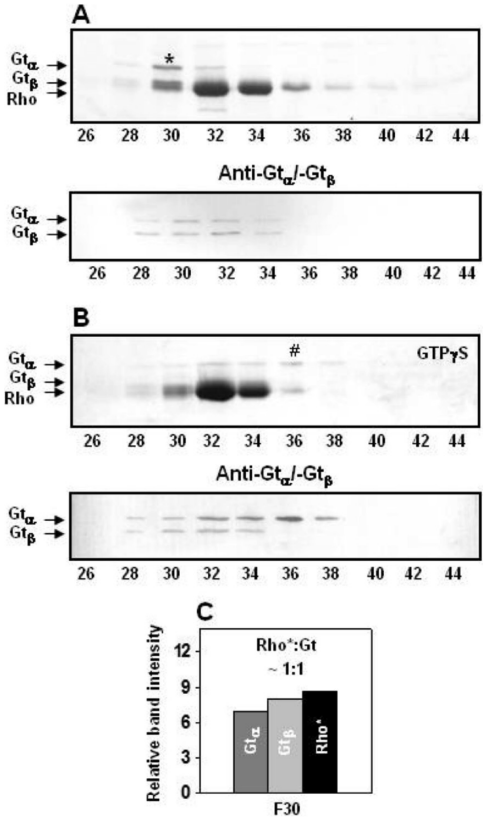

FIGURE 7: Purification of the native Rho*−Gt complex solubilized in DDM by gel filtration. (A) The native Rho*−Gt complex, obtained from ROS membranes and isolated as described in Materials and Methods, was subjected to Sephadex gel filtration chromatography. Asterisks denote fractions containing the Rho*−Gt complex. (B) Dissociation of Gt from the Rho*−Gt complex by GTPγS. Number signs denote fractions containing free Gt. Fractions (30 μL) obtained from a gel filtration column were analyzed by Coomassie blue-stained SDS−PAGE (top panels) and by immunoblots developed with a mixture of anti-Gt_α and anti-Gt_β antibodies (bottom panels). (C) Quantification of band intensities corresponding to Gt_α, Gt_β, and Rho* in fraction 30 containing the Rho*−Gt complex. The molar ratio of Rho*:Gt was ~1:1. The experiment was repeated three times.

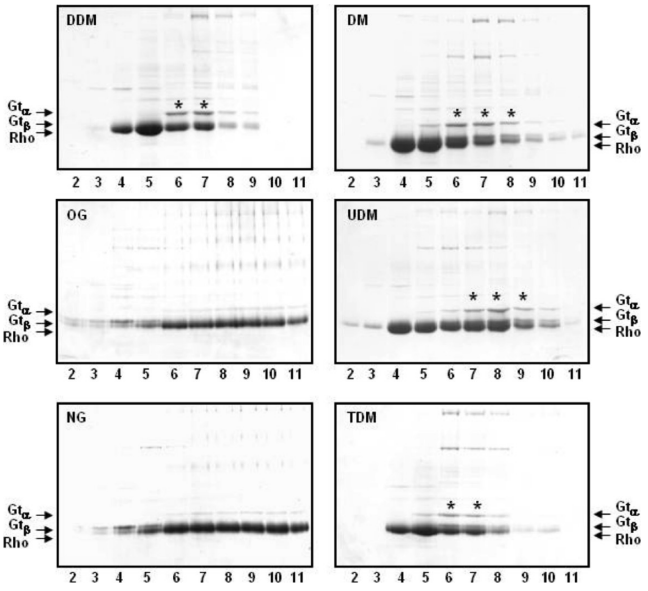

FIGURE 8: Purification of native Rho*−Gt complexes solubilized in different detergents by sucrose gradient ultracentrification. Native Rho*−Gt complexes were prepared from ROS membranes and isolated as described in Materials and Methods. OG, NG, DM, UDM, and TDM in addition to DDM were used for solubilization of the Rho*−Gt complex. Fractions 1−13 (250 μL each) were collected from the top to bottom of sucrose gradients after overnight ultracentrifugation. Fifteen microliters of each fraction was analyzed by Coomassie blue-stained SDS−PAGE. Asterisks denote fractions containing the highest concentrations of the Rho*−Gt complex. Alkyl maltoside detergents (DM, DDM, UDM, and TDM) protected the purified Rho*−Gt complexes and separated them from the excess of illuminated Rho* better than the alkyl glucoside detergents (OG and NG). Presented gels are representative of three independent experiments.

lipid:protein ratio, thereby disrupting formed Rho*−Gt complexes.

For the sake of comparison, reconstituted Rho*−Gt complexes were extracted in a few different detergents such as NG, DM, and TDM and purified by gel filtration in the absence and presence of asolectin (Figure 9). Compared with DDM, Rho in NG and DM migrated in later fractions, most likely because it was present in smaller detergent micelles. In NG, photoactivation clearly shifted migration of some Gt to earlier, heavier fractions (*28*−*30*), probably because of aggregation caused by this detergent. Aggregation of nonactivated Gt in the presence of NG has been observed on a native PAGE gel (not shown). Although Rho* can be found in the same early fractions as Gt (*28*−*30*), its concentration is not sufficient to form a stoichiometrically proper complex with Gt. Addition of lipids (asolectin) in the presence of NG failed to stabilize this complex. In DM, there was no shift in the migration of Gt and Rho*, suggesting complex formation; both Rho* and Gt were present in the same fractions as their control standards. However, prior addition of phospholipids caused them both to shift to earlier fractions, suggesting some stabilizing effect of phospholipids on complex formation. More Rho*−Gt complex was formed in TDM because Gt clearly shifted to earlier fractions (*28*−*30*) as compared to control free Gt, and addition of phospholipids caused an even further shift to earlier fractions (*24*−*26*).

DISCUSSION

The visual signaling cascade is initiated when Rho, a prototypical G protein-coupled receptor (GPCR), is activated by a photon of light. Conformational changes that occur in the Rho* structure after photoactivation allow proper binding of its cognate heterotrimeric G protein and catalyze rapid GDP−GTP exchange on the Gt_α subunit (*1*). The mechanism of Rho activation and signal transduction is not fully understood. Determining the structure of the complex between Rho* and Gt would greatly improve our knowledge of GPCR signaling, but before this goal can be achieved, biochemical characterization of those complexes is needed.

In this study, we examined certain biochemical properties of complexes reconstituted from purified Rho and Gt and compared them with identical properties of native complexes isolated from ROS membranes. We also tested the effects of adding different phospholipids and using various detergents for Rho*−Gt complex extraction on the stability of the purified complexes.

Formation of a Complex with Purified Components (Rho and Gt). The yield of the Rho*−Gt complex reconstituted by mixing the two purified proteins in the presence of DDM was poor. One factor that may have affected efficient coupling of Gt to purified Rho is the presence of detergent micelles. Although Rho* solubilized in detergent solution can activate Gt, formation

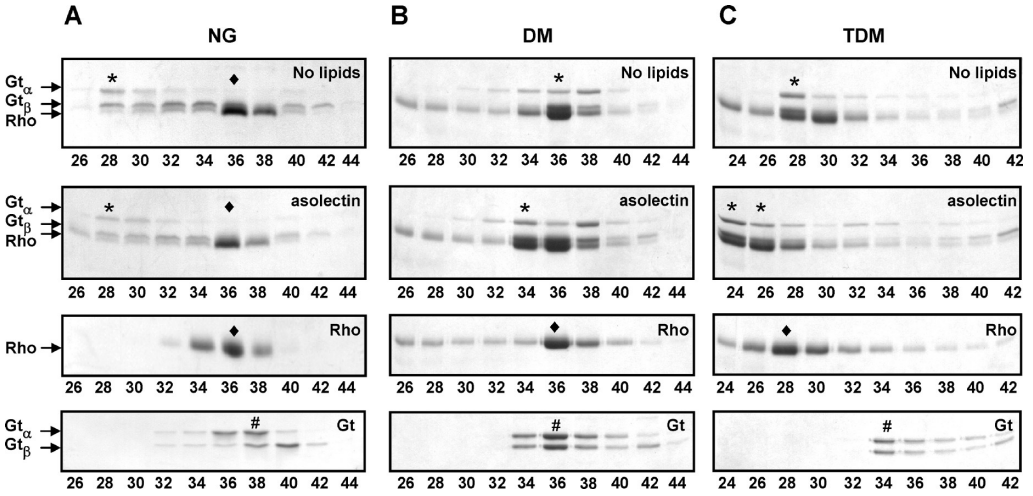

FIGURE 9: Gel filtration of Rho*−Gt complexes, free Rho, and free Gt in NG (A), DM (B), or TDM (C) in the absence or presence of asolectin. Fractions (30 μL) obtained by gel filtration were analyzed by Coomassie blue-stained SDS-PAGE. Asterisks denote fractions containing the Rho*−Gt complex. Number signs denote fractions containing free Gt. Diamonds denote fractions containing free Rho. Presented gels are representative of three independent experiments.

of a stable complex seems to be significantly attenuated. After light illumination, we observed that both Rho* and Gt migrated toward earlier, heavier fractions after gel filtration as compared to free Rho and Gt standards. Quantification of proteins in these fractions revealed that they contained excess Gt, suggesting that some oligomers and aggregates of Gt were formed. Although the effect of activated Rho* on Gt oligomerization has yet to be reported, oligomerization of Gt in solution has been observed (*60*−*62*). Mixing increasing concentrations of Rho* with Gt resulted in higher complex stability with a ratio of 1:1 in the Rho*−Gt complex, but AFM studies have shown that Rho exists in native ROS disk membranes as highly organized and densely packed dimers (*12*, *25*−*27*, *63*). Other biochemical and biophysical studies (*59*, *64*, *65*) as well as estimates that account for the sizes of both Rho and Gt indicate that two molecules of Rho per one Gt are present in the stable complex. Although one Rho per Gt is sufficient to produce a response in the brain, the second Rho molecule in the dimer most likely serves as a platform for proper Gt docking (*37*).

Effect of Phospholipids on the Complex. In ROS membranes, Rho is incorporated into the lipid bilayer (~60 phospholipids per one Rho molecule) (*22*, *23*) where phospholipids tightly surrounding Rho most likely stabilize its oligomeric organization (*52*). Both the headgroups and acyl chains of phospholipids have a significant effect on Meta II formation (*66*−*68*) and G protein anchoring (*69*−*71*). It has been observed that phosphatidylethanolamine (PE) and negatively charged phosphatidylserine (PS), especially with polyunsaturated hydrocarbon side chains, favor the formation of Meta II. Enhanced binding affinity of Gt for Rho* in the presence of phosphatidylethanolamine (PE) has been reported as well (*72*, *73*), but replacement of fatty acids in the lipid matrix of rat ROS membranes reduced not only the level of Rho activation but also Rho*−Gt coupling and PDE activity (*74*). Therefore, the composition of the lipid matrix is critical not only for Rho function but also for the entire process of signal transduction. Here we tested the effect of asolectin, DOPC, DOPE, and DOPS on the binding of Rho* to Gt. Rho and Gt were incubated together with each of these phospholipids before light illumination, and formation of the complex after photoactivation was examined by gel filtration. Compared to controls (free proteins), migration of both Gt and Rho* was shifted to the earlier, heavier fractions, suggesting that coupling had occurred. DOPS had the strongest effect in this regard. This is not surprising because negatively charged PS derivatives reportedly are far more critical for Gt membrane anchoring than uncharged PC (*71*). The ratio of Rho* to Gt in the presence of phospholipids was changed to more than 2:1, indicative of Rho* excess in fractions containing the Rho*−Gt complex. However, when this phospholipid-stabilized complex was subjected again to gel filtration, partial dissociation of the complex occurred unless excess phospholipids were added beforehand (not shown). The stability of the Rho dimer is critically affected by increasing concentrations of detergent, but phospholipids have a stabilizing effect on Rho oligomeric organization (*52*, *57*). Phospholipids may provide a native-like hydrophobic environment for better incorporation of the Rho dimer, or they may interact with detergent micelles, causing a decreased detergent concentration and stimulating Rho self-association (*59*). But if there are not enough phospholipids surrounding Rho, inverted Rho dimers that affect proper Gt binding and decrease the yield of the Rho*−Gt complex can be formed (*41*). Formation of inverted dimers is a consequence of nonspecific interactions between two monomers, so that adequate binding of phospholipids to protein may hinder formation of these structures and stabilize proper parallel dimer conformations.

Phospholipids are also necessary for rapid Gt activation. Although Gt can be activated by Rho* solubilized in detergent, Gt activation was several times faster in the presence of either synthetic phospholipids such as DOPC, DOPE, and DOPS or a mixture of native lipids isolated from ROS membranes. Both DOPS and native lipids provided Gt activation rates similar to those observed when Gt was activated by Rho* in native disk membranes. Thus, these phospholipids most likely stabilize the quaternary structure of Rho for better Gt docking and membrane anchoring that guarantee rapid responses to light and rapid signal transduction.

Comparison of Reconstituted and Native Membrane Complexes between Rho and Gt*. Addition of stabilizing agents such as phospholipids is needed to reconstitute stable complexes of Rho* and Gt from purified components. However, native Rho*−Gt complexes can be isolated directly from ROS membranes wherein phospholipids surrounding Rho have a

good stabilizing effect, on either Rho oligomeric structure, Gt binding, or both. We used two methods to isolate the native complex: gel filtration and sucrose gradient centrifugation. Interestingly, Rho*−Gt complexes isolated by these two procedures had different Rho*:Gt ratios. Although the complex isolated by gel filtration had a 1:1 Rho*:Gt ratio, the complex isolated by sucrose gradient centrifugation displayed a 2:1 Rho*:Gt stoichiometry, similar to that previously reported (*48*). The Rho*−Gt complex purified by sucrose gradient centrifugation was stable over time and migrated in the same fractions after a second sucrose gradient centrifugation (not shown). As confirmed by lipid analysis of the complex-containing fractions collected by gel filtration, the most likely explanation for this discrepancy is that more phospholipids surrounding Rho were removed by gel filtration, resulting in disruption of the Rho* dimeric organization. In contrast, sucrose gradient purification did not expose protein samples to a high volume of detergent-containing buffer, so they retained more phospholipids that protected the Rho oligomeric structure and enhanced Rho*−Gt complex stability. In fact, ~30 phospholipids per Rho* were found in fractions of the complex purified by sucrose gradient ultracentrifugation, whereas only 16 phospholipids per Rho* were quantified in the fractions purified by gel filtration. Thus, a considerably smaller amount of lipid was detected in the reconstituted complex isolated by gel filtration. We also found that the type and concentration of phospholipids and detergent have a strong influence on complex formation.

Effect of Detergents on Rho and Gt Coupling Stability. The detergent used for solubilization of the Rho*−Gt complex had a significant impact on its stability. A few commonly used nonionic detergents that included alkyl glucosides and alkyl maltosides illustrate this effect. All alkyl maltosides employed (DM, UDM, and TDM) seemed to preserve native Rho*−Gt complexes isolated by sucrose gradient centrifugation similar to DDM, whereas alkyl glucosides destroyed these complexes. Differing results most likely were caused by different amounts of phospholipids extracted by the various detergents. Indeed, it was shown that fewer phospholipids were extracted by OG as compared to other detergents during solubilization of Rho from disk membranes (*23*). In other studies in which OG was used for solubilization of the 5-HT_{1A} receptor, 15% less lipid was co-extracted as compared to DDM (*75*). Different effects of different detergents on reconstitution of the Rho*−Gt complex have been noted as well.

CONCLUSIONS

Different complexes of Rho* and Gt were reconstituted with different Rho*:Gt molar ratios. The binding of Gt to Rho* strongly depends on the type of detergent used for Rho solubilization and the amount of co-extracted phospholipids. The presence of phospholipids greatly enhanced the formation and stability of the Rho*−Gt complex. Accordingly, native Rho*−Gt complexes with a Rho*:Gt ratio of 2:1 can be isolated from ROS membranes, where Rho is properly organized and surrounded by native lipids that provide an environment critical for efficient coupling of Gt to Rho*.

ACKNOWLEDGMENT

We thank Dr. Leslie T. Webster, Jr., and members of K.P.'s laboratory for valuable comments on the manuscript.

SUPPORTING INFORMATION AVAILABLE

Spectral properties of Rho (Figure 1S) and gel filtration of free Rho in DDM without and with designated added phospholipids. This material is available free of charge via the Internet at http://pubs.acs.org.

REFERENCES

1. Gilman, A. G. (1987) G proteins: Transducers of receptor-generated signals. *Ann. Rev. Biochem. 56*, 615–649.
2. Oldham, W. M., and Hamm, H. E. (2008) Heterotrimeric G protein activation by G-protein-coupled receptors. *Nat. Rev. Mol. Cell Biol. 9*, 60–71.
3. Tesmer, J. J., and Sprang, S. R. (1998) The structure, catalytic mechanism and regulation of adenylyl cyclase. *Curr. Opin. Struct. Biol. 8*, 713–719.
4. Hamm, H. E., and Gilchrist, A. (1996) Heterotrimeric G proteins. *Curr. Opin. Cell Biol. 8*, 189–196.
5. Palczewski, K. (2006) G protein-coupled receptor rhodopsin. *Ann. Rev. Biochem. 75*, 743–767.
6. Ridge, K. D., and Palczewski, K. (2007) Visual rhodopsin sees the light: Structure and mechanism of G protein signaling. *J. Biol. Chem. 282*, 9297–9301.
7. Leskov, I. B., Klenchin, V. A., Handy, J. W., Whitlock, G. G., Govardovskii, V. I., Bownds, M. D., Lamb, T. D., Pugh, E. N.Jr., and Arshavsky, V. Y. (2000) The gain of rod phototransduction: Reconciliation of biochemical and electrophysiological measurements. *Neuron 27*, 525–537.
8. Bornancin, F., Pfister, C., and Chabre, M. (1989) The transitory complex between photoexcited rhodopsin and transducin. Reciprocal interaction between the retinal site in rhodopsin and the nucleotide site in transducin. *Eur. J. Biochem. 184*, 687–698.
9. Goc, A., Angel, T. E., Jastrzebska, B., Wang, B., Wintrode, P. L., and Palczewski, K. (2008) Different Properties of the Native and Reconstituted Heterotrimeric G Protein Transducin. *Biochemistry 47*, 12409–12419.
10. Angers, S., Salahpour, A., and Bouvier, M. (2001) Biochemical and biophysical demonstration of GPCR oligomerization in mammalian cells. *Life Sci. 68*, 2243–2250.
11. Breitwieser, G. E. (2004) G protein-coupled receptor oligomerization: Implications for G protein activation and cell signaling. *Circ. Res. 94*, 17–27.
12. Fotiadis, D., Jastrzebska, B., Philippsen, A., Muller, D. J., Palczewski, K., and Engel, A. (2006) Structure of the rhodopsin dimer: A working model for G-protein-coupled receptors. *Curr. Opin. Struct. Biol. 16*, 252–259.
13. Muller, D. J., Wu, N., and Palczewski, K. (2008) Vertebrate membrane proteins: Structure, function, and insights from biophysical approaches. *Pharmacol. Rev. 60*, 43–78.
14. Heymann, J. B., Muller, D. J., Mitsuoka, K., and Engel, A. (1997) Electron and atomic force microscopy of membrane proteins. *Curr. Opin. Struct. Biol. 7*, 543–549.
15. Walz, T., Tittmann, P., Fuchs, K. H., Muller, D. J., Smith, B. L., Agre, P., Gross, H., and Engel, A. (1996) Surface topographies at subnanometer-resolution reveal asymmetry and sidedness of aquaporin-1. *J. Mol. Biol. 264*, 907–918.
16. Popot, J. L., Trewhella, J., and Engelman, D. M. (1986) Reformation of crystalline purple membrane from purified bacteriorhodopsin fragments. *EMBO J. 5*, 3039–3044.
17. Dencher, N. A., Kohl, K. D., and Heyn, M. P. (1983) Photochemical cycle and light-dark adaptation of monomeric and aggregated bacteriorhodopsin in various lipid environments. *Biochemistry 22*, 1323–1334.
18. Corless, J. M., Worniallo, E., and Fetter, R. D. (1994) Three-dimensional membrane crystals in amphibian cone outer segments. 1. Light-dependent crystal formation in frog retinas. *J. Struct. Biol. 113*, 64–86.
19. Corless, J. M., McCaslin, D. R., and Scott, B. L. (1982) Two-dimensional rhodopsin crystals from disk membranes of frog retinal rod outer segments. *Proc. Natl. Acad. Sci. U.S.A. 79*, 1116–1120.
20. Krebs, A., Villa, C., Edwards, P. C., and Schertler, G. F. (1998) Characterisation of an improved two-dimensional p22121 crystal from bovine rhodopsin. *J. Mol. Biol. 282*, 991–1003.
21. Schertler, G. F., and Hargrave, P. A. (1995) Projection structure of frog rhodopsin in two crystal forms. *Proc. Natl. Acad. Sci. U.S.A. 92*, 11578–11582.

22. Calvert, P. D., Govardovskii, V. I., Krasnoperova, N., Anderson, R. E., Lem, J., and Makino, C. L. (2001) Membrane protein diffusion sets the speed of rod phototransduction. *Nature 411*, 90–94
23. Aveldano, M. I. (1995) Phospholipid solubilization during detergent extraction of rhodopsin from photoreceptor disk membranes. *Arch. Biochem. Biophys. 324*, 331–343.
24. Nickell, S., Park, P. S., Baumeister, W., and Palczewski, K. (2007) Three-dimensional architecture of murine rod outer segments determined by cryoelectron tomography. *J. Cell Biol. 177*, 917–925.
25. Fotiadis, D., Liang, Y., Filipek, S., Saperstein, D. A., Engel, A., and Palczewski, K. (2003) Atomic-force microscopy: Rhodopsin dimers in native disc membranes. *Nature 421*, 127–128.
26. Fotiadis, D., Liang, Y., Filipek, S., Saperstein, D. A., Engel, A., and Palczewski, K. (2004) The G protein-coupled receptor rhodopsin in the native membrane. *FEBS Lett. 564*, 281–288
27. Liang, Y., Fotiadis, D., Maeda, T., Maeda, A., Modzelewska, A., Filipek, S., Saperstein, D. A., Engel, A., and Palczewski, K. (2004) Rhodopsin signaling and organization in heterozygote rhodopsin knockout mice. *J. Biol. Chem. 279*, 48189–48196
28. Chan, F., Bradley, A., Wensel, T. G., and Wilson, J. H. (2004) Knock-in human rhodopsin-GFP fusions as mouse models for human disease and targets for gene therapy. *Proc. Natl. Acad. Sci. U.S.A. 101*, 9109–9114
29. Chabre, M., and le Maire, M. (2005) Monomeric G-protein-coupled receptor as a functional unit. *Biochemistry 44*, 9395–9403.
30. Baylor, D. (1996) How photons start vision. *Proc. Natl. Acad. Sci. U. S.A. 93*, 560–565.
31. Whorton, M. R., Jastrzebska, B., Park, P. S., Fotiadis, D., Engel, A., Palczewski, K., and Sunahara, R. K. (2008) Efficient coupling of transducin to monomeric rhodopsin in a phospholipid bilayer. *J. Biol. Chem. 283*, 4387–4394.
32. Bayburt, T. H., Leitz, A. J., Xie, G., Oprian, D. D., and Sligar, S. G. (2007) Transducin activation by nanoscale lipid bilayers containing one and two rhodopsins. *J. Biol. Chem. 282*, 14875–14881.
33. Banerjee, S., Huber, T., and Sakmar, T. P. (2008) Rapid incorporation of functional rhodopsin into nanoscale apolipoprotein bound bilayer (NABB) particles. *J. Mol. Biol. 377*, 1067–1081.
34. Ernst, O. P., Gramse, V., Kolbe, M., Hofmann, K. P., and Heck, M. (2007) Monomeric G protein-coupled receptor rhodopsin in solution activates its G protein transducin at the diffusion limit. *Proc. Natl. Acad. Sci. U.S.A. 104*, 10859–10864.
35. Lambright, D. G., Sondek, J., Bohm, A., Skiba, N. P., Hamm, H. E., and Sigler, P. B. (1996) The 2.0 Å crystal structure of a heterotrimeric G protein. *Nature 379*, 311–319.
36. Ciarkowski, J., Witt, M., and Slusarz, R. (2005) A hypothesis for GPCR activation. *J. Mol. Model. 11*, 407–415.
37. Filipek, S., Krzysko, K. A., Fotiadis, D., Liang, Y., Saperstein, D. A., Engel, A., and Palczewski, K. (2004) A concept for G protein activation by G protein-coupled receptor dimers: The transducin/rhodopsin interface. *Photochem. Photobiol. Sci. 3*, 628–638.
38. Filizola, M., Olmea, O., and Weinstein, H. (2002) Prediction of heterodimerization interfaces of G-protein coupled receptors with a new subtractive correlated mutation method. *Protein Eng. 15*, 881–885.
39. Fanelli, F., and De Benedetti, P. G. (2005) Computational modeling approaches to structure-function analysis of G protein-coupled receptors. *Chem. Rev. 105*, 3297–3351.
40. Wen, X. H., Shen, L., Brush, R. S., Michaud, N., Al-Ubaidi, M. R., Gurevich, V. V., Hamm, H. E., Lem, J., Dibenedetto, E., Anderson, R. E., and Makino, C. L. (2009) Overexpression of rhodopsin alters the structure and photoresponse of rod photoreceptors. *Biophys. J. 96*, 939–950
41. Palczewski, K., Kumasaka, T., Hori, T., Behnke, C. A., Motoshima, H., Fox, B. A., Le Trong, I., Teller, D. C., Okada, T., Stenkamp, R. E., Yamamoto, M., and Miyano, M. (2000) Crystal structure of rhodopsin: A G protein-coupled receptor. *Science 289*, 739–745
42. Okada, T., Le Trong, I., Fox, B. A., Behnke, C. A., Stenkamp, R. E., and Palczewski, K. (2000) X-ray diffraction analysis of three-dimensional crystals of bovine rhodopsin obtained from mixed micelles. *J. Struct. Biol. 130*, 73–80
43. Mustafi, D., and Palczewski, K. (2008) Topology of class A G protein-coupled receptors: Insights gained from crystal structures of rhodopsins, adrenergic and adenosine receptors. *Mol. Pharmacol.* XXXX (in press)
44. Rosenbaum, D. M., Cherezov, V., Hanson, M. A., Rasmussen, S. G., Thian, F. S., Kobilka, T. S., Choi, H. J., Yao, X. J., Weis, W. I., Stevens, R. C., and Kobilka, B. K. (2007) GPCR engineering yields high-resolution structural insights into β2-adrenergic receptor function. *Science 318*, 1266–1273.
45. Hanson, M. A., and Stevens, R. C. (2009) Discovery of New GPCR Biology: One Receptor Structure at a Time. *Structure 17*, 8–14.
46. Fukada, Y., Takao, T., Ohguro, H., Yoshizawa, T., Akino, T., and Shimonishi, Y. (1990) Farnesylated γ-subunit of photoreceptor G protein indispensable for GTP binding. *Nature 346*, 658–660.
47. Kokame, K., Fukada, Y., Yoshizawa, T., Takao, T., and Shimonishi, Y. (1992) Lipid modification at the N terminus of photoreceptor G-protein α-subunit. *Nature 359*, 749–752.
48. Jastrzebska, B., Golczak, M., Fotiadis, D., Engel, A., and Palczewski, K. (2009) Isolation and functional characterization of a stable complex between photoactivated rhodopsin and the G protein, transducin. *FASEB J. 23*, 371–381.
49. Papermaster, D. S. (1982) Preparation of retinal rod outer segments. *Methods Enzymol. 81*, 48–52.
50. Wald, G., and Brown, P. K. (1953) The molecular excitation of rhodopsin. *J. Gen. Physiol. 37*, 189–200
51. Bradford, M. M. (1976) A rapid and sensitive method for the quantitation of microgram quantities of protein utilizing the principle of protein-dye binding. *Anal. Biochem. 72*, 248–254.
52. Jastrzebska, B., Fotiadis, D., Jang, G. F., Stenkamp, R. E., Engel, A., and Palczewski, K. (2006) Functional and structural characterization of rhodopsin oligomers. *J. Biol. Chem. 281*, 11917–11922
53. Heck, M., and Hofmann, K. P. (2001) Maximal rate and nucleotide dependence of rhodopsin-catalyzed transducin activation: Initial rate analysis based on a double displacement mechanism. *J. Biol. Chem. 276*, 10000–10009
54. Fahmy, K., Jager, F., Beck, M., Zvyaga, T. A., Sakmar, T. P., and Siebert, F. (1993) Protonation states of membrane-embedded carboxylic acid groups in rhodopsin and metarhodopsin II: A Fourier-transform infrared spectroscopy study of site-directed mutants. *Proc. Natl. Acad. Sci. U.S.A. 90*, 10206–10210
55. Folch, J., Lees, M., and Sloane Stanley, G. H. (1957) A simple method for the isolation and purification of total lipides from animal tissues. *J. Biol. Chem. 226*, 497–509
56. White, D. C., and Ringleberg, D. B. (1995) Signature Lipid Biomarker Analysis , Oxford University Press, New York.
57. Jastrzebska, B., Maeda, T., Zhu, L., Fotiadis, D., Filipek, S., Engel, A., Stenkamp, R. E., and Palczewski, K. (2004) Functional characterization of rhodopsin monomers and dimers in detergents. *J. Biol. Chem. 279*, 54663–54675.
58. Preininger, A. M., and Hamm, H. E. (2004) G protein signaling: insights from new structures. *Sci. STKE 2004 (218)*, re3.
59. Mansoor, S. E., Palczewski, K., and Farrens, D. L. (2006) Rhodopsin self-associates in asolectin liposomes. *Proc. Natl. Acad. Sci. U.S.A. 103*, 3060–3065.
60. Baehr, W., Morita, E. A., Swanson, R. J., and Applebury, M. L. (1982) Characterization of bovine rod outer segment G-protein. *J. Biol. Chem. 257*, 6452–6460
61. Hingorani, V. N., Tobias, D. T., Henderson, J. T., and Ho, Y. K. (1988) Chemical cross-linking of bovine retinal transducin and cGMP phosphodiesterase. *J. Biol. Chem. 263*, 6916–6926
62. Vaillancourt, R. R., Dhanasekaran, N., Johnson, G. L., and Ruoho, A. E. (1990) 2-Azido-[^{32}P]NAD$^+$, a photoactivatable probe for G-protein structure: Evidence for holotransducin oligomers in which the ADP-ribosylated carboxyl terminus of α interacts with both α and γ subunits. *Proc. Natl. Acad. Sci. U.S.A. 87*, 3645–3649
63. Liang, Y., Fotiadis, D., Filipek, S., Saperstein, D. A., Palczewski, K., and Engel, A. (2003) Organization of the G protein-coupled receptors rhodopsin and opsin in native membranes. *J. Biol. Chem. 278*, 21655–21662.
64. Kota, P., Reeves, P. J., Rajbhandary, U. L., and Khorana, H. G. (2006) Opsin is present as dimers in COS1 cells: Identification of amino acids at the dimeric interface. *Proc. Natl. Acad. Sci. U.S.A. 103*, 3054–3059.
65. Suda, K., Filipek, S., Palczewski, K., Engel, A., and Fotiadis, D. (2004) The supramolecular structure of the GPCR rhodopsin in solution and native disc membranes. *Mol. Membr. Biol. 21*, 435–446.
66. Wiedmann, T. S., Pates, R. D., Beach, J. M., Salmon, A., and Brown, M. F. (1988) Lipid-protein interactions mediate the photochemical function of rhodopsin. *Biochemistry 27*, 6469–6474
67. Gibson, N. J., and Brown, M. F. (1993) Lipid headgroup and acyl chain composition modulate the MI-MII equilibrium of rhodopsin in recombinant membranes. *Biochemistry 32*, 2438–2454
68. Brown, M. F. (1994) Modulation of rhodopsin function by properties of the membrane bilayer. *Chem. Phys. Lipids 73*, 159–180
69. Vogler, O., Casas, J., Capo, D., Nagy, T., Borchert, G., Martorell, G., and Escriba, P. V. (2004) The G$\beta\gamma$ dimer drives the interaction of heterotrimeric Gi proteins with nonlamellar membrane structures. *J. Biol. Chem. 279*, 36540–36545.

70. Mitchell, D. C., Niu, S. L., and Litman, B. J. (2001) Optimization of receptor-G protein coupling by bilayer lipid composition I: Kinetics of rhodopsin-transducin binding. *J. Biol. Chem. 276*, 42801–42806.
71. Kosloff, M., Alexov, E., Arshavsky, V. Y., and Honig, B. (2008) Electrostatic and lipid anchor contributions to the interaction of transducin with membranes: Mechanistic implications for activation and translocation. *J. Biol. Chem. 283*, 31197–31207.
72. Alves, I. D., Salgado, G. F., Salamon, Z., Brown, M. F., Tollin, G., and Hruby, V. J. (2005) Phosphatidylethanolamine enhances rhodopsin photoactivation and transducin binding in a solid supported lipid bilayer as determined using plasmon-waveguide resonance spectroscopy. *Biophys. J. 88*, 198–210.
73. Wang, Y., Botelho, A. V., Martinez, G. V., and Brown, M. F. (2002) Electrostatic properties of membrane lipids coupled to metarhodopsin II formation in visual transduction. *J. Am. Chem. Soc. 124*, 7690–7701.
74. Niu, S. L., Mitchell, D. C., Lim, S. Y., Wen, Z. M., Kim, H. Y., Salem, N.Jr., and Litman, B. J. (2004) Reduced G protein-coupled signaling efficiency in retinal rod outer segments in response to n-3 fatty acid deficiency. *J. Biol. Chem. 279*, 31098–31104.
75. Banerjee, P., Joo, J. B., Buse, J. T., and Dawson, G. (1995) Differential solubilization of lipids along with membrane proteins by different classes of detergents. *Chem. Phys. Lipids 77*, 65–78.